Dear author,

Please note that changes made in the online proofing system will be added to the article before publication but are not reflected in this PDF.

We also ask that this file not be used for submitting corrections.

Available online at www.sciencedirect.com

ScienceDirect

journal homepage: www.elsevier.com/locate/he

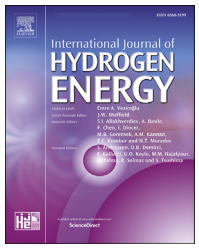

Study of Ni/CeO_2–ZnO catalysts in the production of H_2 from acetone steam reforming

K.F.M. Elias [a], L. Bednarczuk [b], E.M. Assaf [a], P. Ramírez de la Piscina [b], N. Homs [b,c,*]

[a] Instituto de Química de São Carlos, Universidade de São Paulo, Av. Trab. São-Carlense, 400 – Parque Arnold Schmidt, São Carlos – SP 13566-590, Brazil

[b] Departament de Química Inorgànica I Orgànica, Secció Química Inorgànica and Institut de Nanociència I Nanotecnologia (IN2UB), Universitat de Barcelona, Martí I Franquès 1, 08028 Barcelona, Spain

[c] Institut de Recerca en Energia de Catalunya (IREC), Jardins de Les Dones de Negre 1, 08930 Barcelona, Spain

ARTICLE INFO

Article history:
Received 11 July 2018
Received in revised form
22 October 2018
Accepted 24 October 2018
Available online xxx

Keywords:
H_2 from acetone
ASR
Ni-based catalysts
NiZn alloy
ZnO–CeO_2 support
Coke

ABSTRACT

This paper reports the study of new Ni/ZnO-based catalysts for hydrogen production from substoichiometric acetone steam reforming (ASR). The effect of CeO_2 introduction is analyzed regarding the catalytic behavior and carbon deposits formation. ASR was studied at 600 °C using a steam/carbon ratio S/C = 1. Ni/xCeZnO (x = 10, 20, 30 CeO_2 wt %) catalysts showed a better performance than the bare Ni/ZnO. Ni/xCeZnO generated a lower amount and less ordered carbon deposits than Ni/ZnO. The higher the CeO_2 content in Ni/xCeZnO, the lower the amount of carbon deposits in the post-reaction catalyst. The highest H_2 production under ASR at the experimental conditions used was achieved for the Ni/xCeZnO catalysts. *In-situ* DRIFTS-MS experiments under ESR conditions showed different reaction pathways over Ni/20CeZnO and Ni/ZnO catalysts.

Introduction

The production of hydrogen from biomass-derived substrates is of current interest due to the concerns of CO_2 global emissions. Biomass-derived oxygenates such as alcohols are the most studied H_2-carriers [1]. Particularly, the H_2 production from ethanol has been extensively studied due to its actual production and easy handle [2]. The ethanol steam reforming (ESR) can give up to 6 mol of H_2 per mole of ethanol converted. However, depending on the catalysts used, the ESR gives besides H_2 and CO_2 several by-products such as CH_4, CO and C2+ compounds such as ethylene and acetone, which diminish the H_2-yield [3]. Moreover, the formation of these C2+ compounds has been related to the formation of carbon deposits, which could produce the deactivation of the catalyst [3,4]. In this context and for preventing the catalyst deactivation, the study of acetone steam reforming (ASR) is of great interest.

* *Corresponding author*. Departament de Química Inorgànica I Orgànica, Secció Química Inorgànica and Institut de Nanociència I Nanotecnologia (IN2UB), Universitat de Barcelona, Martí I Franquès 1, 08028 Barcelona, Spain.
E-mail address: narcis.homs@qi.ub.edu (N. Homs).

https://doi.org/10.1016/j.ijhydene.2018.10.191
0360-3199/

Please cite this article as: Elias KFM et al., Study of Ni/CeO_2–ZnO catalysts in the production of H_2 from acetone steam reforming, International Journal of Hydrogen Energy, https://doi.org/10.1016/j.ijhydene.2018.10.191

$CH_3COCH_{3(g)} + 5H_2O_{(g)} \leftrightarrow 3CO_{2(g)} + 8H_{2(g)}$
$\Delta H^{\circ}_{298\ K} = 246.3\ kJ\ mol^{-1}$

Moreover, acetone is used as a model molecule for the study of bio-oil steam reforming to H_2 [5–8], and plays a role in the reforming of several oxygenate subtracts such as acetic acid [6–9]. However, the ASR has been much less studied than ESR [1].

Different transition metal-based catalysts have been used for the steam reforming of oxygenates. Besides noble metals, Ni, Co have been largely studied as active phases regarding their ability to break C–C, C–H and C–O bonds. Both Co and Ni have been proved to be effective for steam reforming of C2 and C3 oxygenate substrates, i.e. ethanol, glycerol among others [1,3,10,11]. Nowadays, exists interest in the use Ni-based catalysts for reforming processes of oxygenate subtracts due to their widely recognized application for hydrocarbon steam reforming processes, their cost and availability [5,6,11].

Besides the metallic active phase, the composition and nature of the support plays a major role in steam reforming processes [1,3,10,11]. We have recently reported the effect of the support on the carbon deposits formed under sub-stoichiometric ESR conditions over Ni-based catalysts [12].

ZnO has been extensively used in the past as support of Co-based catalysts for efficient ESR processes [10]. On the other hand, it is well-known that CeO_2 plays a main role associated with the presence of oxygen vacancies [11,13].

In the present work, we report a study of new Ni-based catalysts focusing on the effect of CeO_2 in Ni/ZnO-based catalysts for H_2 production from ASR. The catalysts were deeply characterized before and after use, and their characteristics correlated with their performance in ASR under sub-stoichiometric conditions (H_2O/acetone = 3 M, steam to carbon ratio (S/C) = 1). For such purposes, X-ray diffraction (XRD), oxygen storage capacity (OSC), H_2-temperature programmed reduction (H_2-TPR) and Raman spectroscopy analysis of the catalysts were carried out; the reduction process was followed by *in-situ* XRD analysis at the Brazilian synchrotron facilities. Moreover, *in-situ* DRIFTS-MS experiments under ESR conditions were carried out with several samples.

Materials and Methods

Catalyst preparation and characterization

Catalysts were prepared by the co-precipitation method using aqueous solutions of Ni^{2+}, Ce^{3+} and Zn^{2+} nitrates and sodium carbonate as precipitating agent. After filtration and thorough washing with water, the precipitates were dried at 85 °C and calcined at 600 °C. The Ni content was kept about 10 wt%, and the catalysts were labelled: Ni/ZnO and Ni/xCeZnO, where x stands for the wt% of CeO_2 (x = 10, 20 and 30).

The chemical composition of the catalysts was determined by inductively-coupled plasma atomic emission spectrometry using an ICP-OES Perkin Elmer Optima 3200RL equipment. N_2 adsorption-desorption BET isotherms were recorded at −196 °C using a Micromeritics Tristar-II. The specific surface area (S_{BET}) was calculated by multi-point BET analysis of the nitrogen adsorption isotherms.

Raman spectroscopy was performed using a Jobin-Yvon LabRam HR 800, fitted to an optical Olympus BXFM microscope with a CCD detector cooled to −70 °C and a 532 nm laser. XRD patterns catalysts were recorded using a Siemens D-500 X-ray diffractometer with nickel-filtered $CuK_{\alpha 1}$ radiation. The XRD profiles were collected between $2\theta = 20°$ and 100°, with a step width of 0.05° counting 3 s at each step. The mean crystallite size of the particles was calculated according to the Debye-Scherrer equation. On the other hand, the reduction process under H_2 up to 700 °C was followed by *in-situ* XRD at the Brazilian Synchrotron Light Laboratory (LNLS) at Campinas (Brazil).

The oxygen storage capacity of the catalysts (OSC) was measured using a Sensys Evo DSC instrument (Setaram) equipped with a 3D thermal flow sensor. Before analysis, the samples (50 mg) were reduced with H_2/Ar (12%, vol/vol); the temperature was linearly increased at 10 °C/min up to 800 °C and was kept at 800 °C during 5 min. Then, they were cooled to 300 °C under Ar flow. A stream of O_2/He (10% vol/vol) was periodically injected into the reduced sample until saturation and accordingly the consumption of oxygen was calculated.

H_2-TPR experiments were performed using a Micromeritics AutoChem II 5920 analyser. The sample (40 mg) was exposed to a flow of H_2/Ar (12% v/v), and the temperature was linearly increased at 10 °C min^{-1} up to 800 °C.

In-situ DRIFTS-MS experiments were carried out under ESR conditions (water/ethanol vapour ratio of 6 mol/mol) using a Bruker Vertex 70 spectrophotometer equipped with a liquid nitrogen-cooled MCT detector, a DRIFTS catalytic chamber and coupled to a ThermoStar mass spectrometer. The recorded spectra consisted of 128 scans at a spectral resolution of 4 cm^{-1} and corrected with the subtraction of adsorbed water spectrum.

Catalytic tests

Catalytic tests were carried out under atmospheric pressure in a continuous-flow tubular fixed-bed stainless steel reactor. The catalyst (200 mg) was mixed with inactive SiC (0.5 mm) up to a catalytic volume of approximately 1 mL. The temperature was measured using a thermocouple in direct contact with the catalytic bed. Before the reaction, the catalyst was *in-situ* reduced under an H_2/Ar 10% vol/vol mixture at 700 °C for 1.5 h; then, the flow switched to Ar and kept at 600 °C. A liquid mixture of water/acetone (molar ratio = 3, S/C = 1) was injected (0.015 ml min^{-1}) using a Gilson 307 pump, evaporated at 200 °C and mixed with a flow of Ar and N_2 (30% v/v of N_2, as internal standard) in a custom-built system, and then directed to the reactor in continuous-flow mode. The catalytic behavior of reduced catalysts was analyzed at 600 °C for 20 h under a gas hourly space velocity (GHSV) of about 7800 h^{-1}; the first data point was taken after 1 h under stream. Besides acetone, gasification products H_2, CO, CO_2 and CH_4 (only traces of C2 and C3 compounds were detected), were on-line analyzed in the reactor effluent using an on-line Bruker 450 GC equipped with TCD and FID detectors; water and heavier products were not quantified. The acetone conversion ($X_{Acetone}$) and the gas phase product distribution, expressed as the molar concentration of the i product (S_i), were calculated as follows:

Please cite this article as: Elias KFM et al., Study of Ni/CeO_2–ZnO catalysts in the production of H_2 from acetone steam reforming, International Journal of Hydrogen Energy, https://doi.org/10.1016/j.ijhydene.2018.10.191

$X_{Acetone}$ (%) = 100(Acetone$_{in}$ − Acetone$_{out}$)/Acetone$_{in}$ and $S_i = n_i/n_{total}$, respectively; where n_i is the number of moles of the i product and n_{total} is the total number of moles of the gaseous products analyzed (H_2, CO, CO_2 and CH_4). The yield of H_2 was referred to the maximum attainable production of H_2 under the substoichiometric ASR conditions used; H_2 yield (%) = 100 × (mol H_2/6 mol Acetone$_{in}$).

The post-reaction catalysts were analyzed by XRD, Raman spectroscopy and temperature programmed oxidation with thermogravimetric-mass spectrometry analysis (TG-TPO-MS). For this experiment, about 50 mg of the spent catalyst previously sieved to separate out the SiC, was treated under an air flow at 10 °C min^{-1} up to 800 °C. The heat flow and mass change were continuously registered and the outlet gases analyzed on-line by an Omnistar (Pfeiffer) mass spectrometer.

Results and discussion

Table 1 shows the chemical composition and several characteristics of the catalysts. The Na content was in all cases <0.1 wt%. The BET areas of Ni/xCeZnO (18–19 m^2g^{-1}) are only slightly higher than that of the bare Ni/ZnO (13 m^2g^{-1}).

From XRD analysis of calcined samples (Fig. 1), besides the presence of ZnO (JCDPS 36-1451) and CeO_2 phases (JCDPS 34-394), the presence of NiO was confirmed. Table 1 also compiles the calculated crystallite size of the NiO phase for the calcined samples. Slightly smaller NiO crystallites were found in Ni/xCeZnO when compared with those in Ni/ZnO.

The OSC values determined for Ni/xCeZnO samples are higher than that of Ni/ZnO (Table 1). For Ni/xCeZnO, the higher the content of CeO_2, the higher the OSC value found.

Fig. 2 shows the Raman spectra in the 50-1000 cm^{-1} range of Ni/ZnO and Ni/xCeZnO catalysts. The spectrum of Ni/ZnO catalyst shows two Raman bands at 100 cm^{-1} and 437 cm^{-1} which are related to the E_2 (low and high, respectively) phonon modes, characteristic of the bulk ZnO [14]. For the Ni/xCeZnO spectra, as the CeO_2 content increases, a progressive diminution of these bands is observed and simultaneously, a rising of a well-defined band located at 460-464 cm^{-1} is clearly visible that is attributed to the optical Raman F_{2g} mode of CeO_2 [15]. Weak intensity Raman shifts in the 200-300 cm^{-1} region are visible for the Ni/20CeZnO and Ni/30CeZnO catalysts, which are ascribed to the second-order Raman features of CeO_2 [15]. Moreover, for Ni/20CeZnO and Ni/30CeZnO catalysts, a low intensity band at about 600 cm^{-1} can be observed. A Raman shift in this position has been related with the presence of oxygen vacancies in the ceria lattice [15,16]; this in good agreement with the determined OSC values.

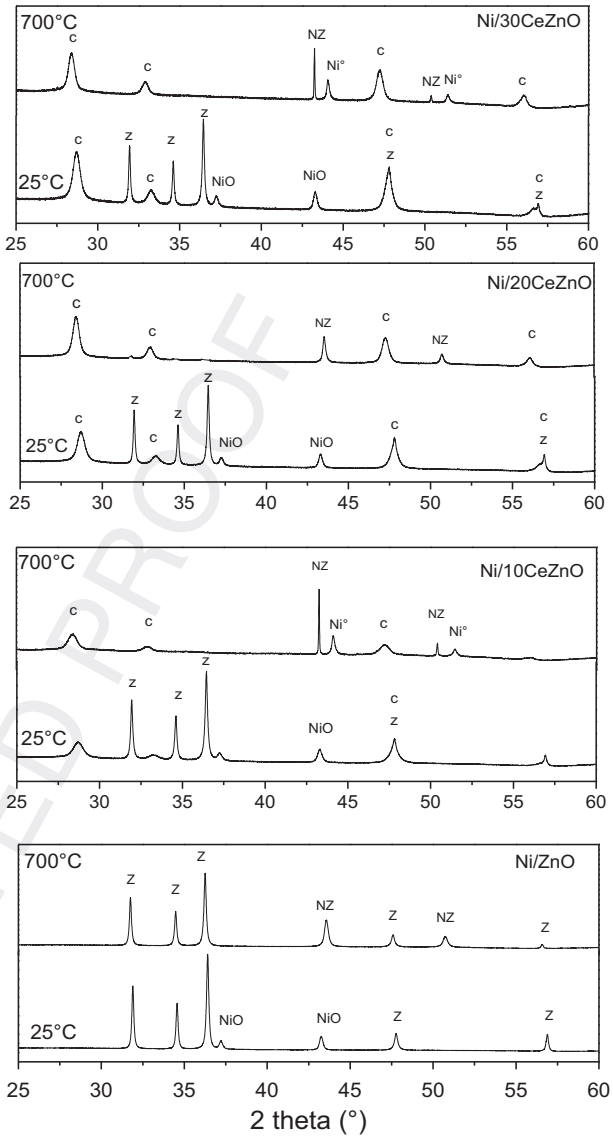

Fig. 1 – XRD at 25 °C of calcined catalysts and after the *in-situ* XRD reduction process from 25 °C up to 700 °C. Phases: Ni°; NiO; C=CeO_2; Z = ZnO and NZ = Ni_xZn_y.

Fig. 3 shows the H_2-TPR profiles registered for the catalysts. All catalysts presented a main H_2-consumption peak with maximum located between 450 °C and 530 °C and a shoulder in the temperature range of 550–750 °C. Peaks in the range 350–450 °C could be assigned to the reduction of NiO, which

Table 1 – Several characteristics of catalysts.

Catalyst	Ni (%wt)	BET (m^2/g)	OSC (μmol/g)	H_2-consumption (mol H_2/mol Ni)	d (nm) (XRD)		
					NiO	Ni_xZn_y	Ni^0
Ni/ZnO	9.75	13	487	1.08	39	27	–
Ni/10CeZnO	9.77	18	509	1.18	27	80	40
Ni/20CeZnO	9.56	19	520	1.19	28	37	–
Ni/30CeZnO	9.47	18	568	1.19	33	97	37

Please cite this article as: Elias KFM et al., Study of Ni/CeO_2–ZnO catalysts in the production of H_2 from acetone steam reforming, International Journal of Hydrogen Energy, https://doi.org/10.1016/j.ijhydene.2018.10.191

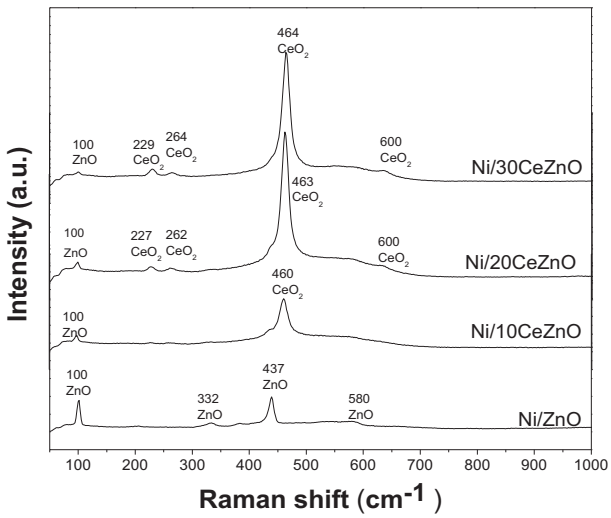

Fig. 2 – Raman spectra of calcined catalysts.

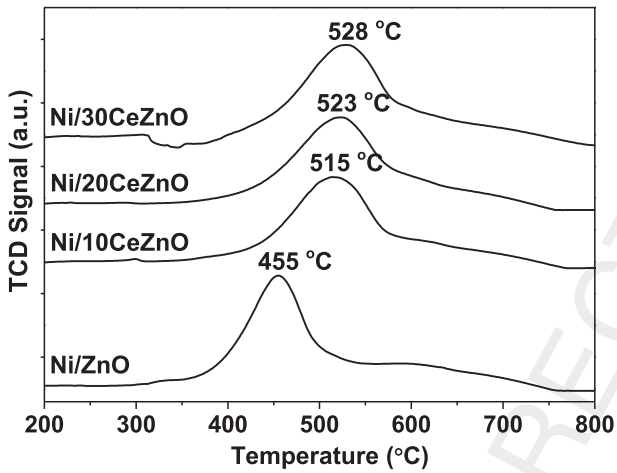

Fig. 3 – Temperature programmed reduction (H_2-TPR) profiles of catalysts.

does not interact with the support [17,18]. An increase in the interaction between Ni^{2+} species and the support produce an increase in the temperature of reduction of Ni^{2+} species [12,19].

The Ni/ZnO catalyst presented the maximum of H_2 consumption at 455 °C. Ni/xCeZnO catalysts showed broad peaks of hydrogen consumption with maximum at a higher temperature (515–528 °C) than that of Ni/ZnO. For Ni/xCeZnO, the higher the CeO_2 content, the higher the temperature of the peak of H_2 consumption. These facts point to the existence of different interactions between the Ni^{2+} species and the support as a function of CeO_2 content. The hydrogen consumption (Table 1), slightly exceeds that expected for the Ni^{2+} reduction ($H_2/Ni^{2+} = 1$ mol/mol), this excess is slightly higher for Ni/xCeZnO than that for Ni/ZnO; this could be related with a partial reduction of the supports.

As stated above, the reduction process was followed by *in-situ* XRD analysis (Fig. 1). In all cases after the H_2-treatment at 700 °C, XRD patterns indicated the disappearance of the NiO and ZnO phases, present at 25 °C for the calcined samples, and the observation of new diffraction peaks at $2\theta = 43.2°$ and 50.4°, which points to the formation of Ni_xZn_y phases (JCDPS 65-5310, JCDPS 47-1019). For Ni/10CeZnO and Ni/30CeZnO catalysts, peaks characteristics of Ni^0 (37 nm and 40 nm, respectively) were also found (Table 1). Table 1 also shows the crystallite size of Ni_xZn_y determined from the *in-situ* XRD analysis. The Ni/ZnO and Ni/20CeZnO catalysts presented smaller Ni_xZn_y crystallite size (27 nm and 37 nm, respectively) than Ni/10ZnO and Ni/30CeZnO (80 nm and 97 nm, respectively).

As stated in the Materials and Methods section, *in-situ* DRIFTS-MS experiments under ESR at 600 °C were carried out over Ni/ZnO and Ni/20CeZnO catalysts. For these experiments, the reduced catalyst was placed in the DRIFTS chamber, firstly pretreated at 600 °C under a H_2/He (12%, vol/vol) flow for 30 min, then cooled down to 120 °C under He flow; further, temperature was raised up to 600 °C, the background spectrum registered and, the flow switched to a He-saturated flow with water/ethanol vapour (6 mol/mol). DRIFT and mass spectra were recorded as a function of time. The *m/z* fragments corresponding to CH_3CH_2OH, CH_3CHO, CH_3COCH_3, CH_3COOH, CH_4, CO_2, CO and H_2 were on-line analyzed by MS. The main products detected during this experiment were H_2, CH_4, CO_2 and acetone. Fig. 4A and B shows the profiles recorded for H_2, CH_4 and acetone in the first 15 min under ESR conditions for both catalysts. As can be seen for Ni/20CeZnO, H_2 and CH_4 evolved initially and negligible acetone formation was detected in the period of analysis (15 min). Contrarily, for Ni/ZnO, the MS analysis during the initial minutes under ESR conditions at 600 °C indicated that, after the initial production of H_2, which occurred in this case at about 10 min under reaction, the evolution of CH_4 and acetone by-products took place. The presence of CeO_2 in the Ni/20CeZnO catalyst could prevent in some extension the formation of acetone under ESR conditions.

The corresponding spectra registered during the *in-situ* DRIFTS analysis under ESR are shown in Fig. 4C. The spectrum of Ni/ZnO catalyst exhibits a set of bands in the 1600-1450 cm^{-1} region which can be related to the modes υ_{as} (COO), υ_s (COO), δ_{as} (CH_3) and δ_s (CH_3) of different surface carboxylate (acetate-type) species (spectrum a in Fig. 4C) [20–24]. Moreover, several bands above 1700 cm^{-1}, e.g. with well-defined maxima at 1742 cm^{-1} and 1701 cm^{-1}, could be related to υ(C=O) vibration of adsorbed acetone and acetaldehyde [25]. However, the broadness of these bands together the presence of other absorptions, as those centered at 1673 cm^{-1} and 1648 cm^{-1}, points to the presence of other unsaturated carbonylic species as 2-butenal [26–31]. Contrarily, the spectrum corresponding to the Ni/20CeZnO catalyst at the same conditions (spectrum b in Fig. 4C) do not shows clear absorptions above 1700 cm^{-1}, but only very low intensity bands related to surface unsaturated carbonylic and carboxylate species. However, a new band centered at 1585 cm^{-1}, which is not present in the case of the Ni/ZnO, is visible. A band at this position has been related with the presence of different carboxylate species (formate type) adsorbed at ZnO [32]. From the DRIFTS results, different surface reaction intermediates are identified for the Ni/ZnO and Ni/20CeZnO catalysts under ESR conditions. This could result in a different evolution of

Please cite this article as: Elias KFM et al., Study of Ni/CeO_2–ZnO catalysts in the production of H_2 from acetone steam reforming, International Journal of Hydrogen Energy, https://doi.org/10.1016/j.ijhydene.2018.10.191

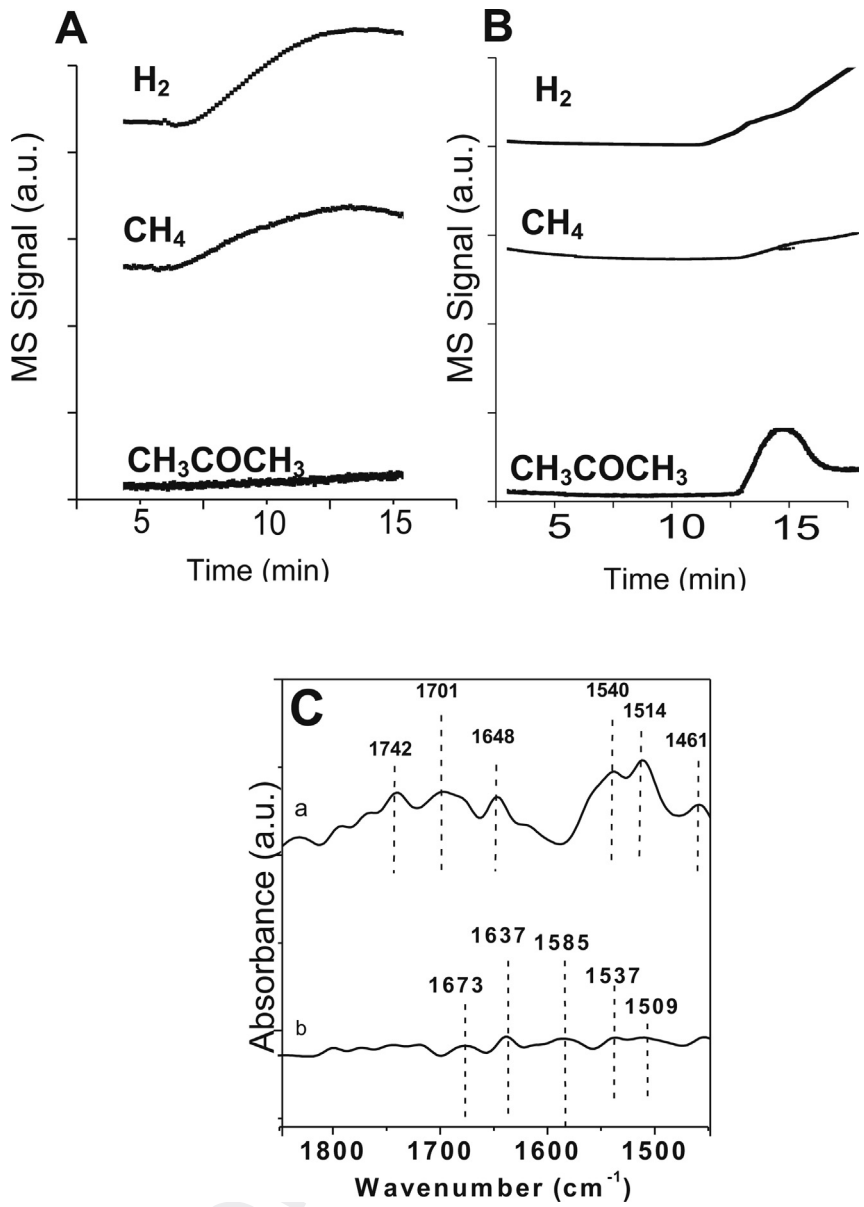

Fig. 4 – *In-situ* DRIFTS-MS results under ESR conditions (T = 600 °C, water/ethanol vapour = 6 mol/mol); A and B, mass spectra profiles of initial evolution of selected products over Ni/ZnO and Ni/20CeZnO catalysts, respectively; C, the corresponding DRIFT spectra registered after 15 min for a) Ni/ZnO and b) Ni/20CeZnO catalysts.

products, as identified by on line MS analysis under ESR at 600 °C. The evolution of surface carboxylates to H_2, CH_4 and CO_2 appears to be the main reaction pathway. However, for Ni/ZnO additional routes of surface species and their further evolution to acetone and unsaturated aldehydes seems to exist. From these results, a less favored route to acetone formation under ESR for the Ni/20CeZnO catalyst than for the bare Ni/ZnO could be proposed. It is well known that acetone can undergo aldol condensation and oligomerization reactions resulting in the formation of coke/oligomer products [5,33]. Under ESR conditions, a less favored route to acetone formation could reduce the carbonaceous deposits formation using Ni/xCeZnO catalysts when compared with Ni/ZnO counterpart.

Finally, the reduced catalysts were tested under sub-stoichiometric ASR conditions (S/C = 1) at 600 °C. Under these conditions, for all catalysts similar initial acetone conversion values were obtained (in all cases below 100%); this allowed a proper comparison of the catalytic behavior of the samples along time (20 h). Table 2 shows the initial and final conversion values obtained for the catalysts under ASR (S/C = 1). As can be seen, despite initial acetone conversion was similar for all catalysts, the Ni/xCeZnO systems showed less deactivation over the reaction time than that observed for the bare Ni/ZnO catalyst. The catalyst that presented the lowest deactivation was Ni/20CeZnO. Table 2 also shows the initial distribution of H_2, CO and CO_2 products (S_i, mol/mol) for the catalysts; minor amounts of CH_4 were found at the ending of the reaction

Please cite this article as: Elias KFM et al., Study of Ni/CeO_2–ZnO catalysts in the production of H_2 from acetone steam reforming, International Journal of Hydrogen Energy, https://doi.org/10.1016/j.ijhydene.2018.10.191

Table 2 – Initial and final acetone conversion ($X_{Acetone}$), H_2 yield and, initial product (H_2, CO, CO_2) distribution (mol/mol) for the catalysts under ASR conditions; T = 600 °C, S/C = 1, GHSV = 7800 h^{-1}, reaction time = 20 h.

Catalyst	$X_{Acetone}$ (%)		H_2	CO	CO_2	H_2 yield (%)	
	INITIAL	FINAL				INITIAL	FINAL
Ni/ZnO	89	75	0.61	0.06	0.33	16.5	9.8
Ni/10CeZnO	82	79	0.76	0.05	0.19	27.3	16.7
Ni/20CeZnO	85	84	0.67	0.05	0.28	24.7	21.6
Ni/30CeZnO	89	81	0.65	0.09	0.26	38.7	30.7

Table 3 – Several characteristics of post-reaction catalysts.

Catalyst	dNi^0 (XRD) (nm)	Raman (I_G/I_D)	Carbonde position ($gC.g_{cat}^{-1}.h^{-1}$)
Ni/ZnO	44	0.60	0.090
Ni/10CeZnO	25	0.55	0.082
Ni/20CeZnO	23	0.50	0.065
Ni/30CeZnO	21	0.43	0.065

period. Although at the initial reaction time the H_2/CO_x ratio is close to the expected for the sub stoichiometric ASR conditions used (ca. 2), this value increased with reaction time. The initial and final hydrogen yield for the catalysts under the substoichiometric ASR conditions appears also compiled in Table 2. These results points that under the ASR (S/C = 1) conditions used, the reforming reaction is only achieved in a minor extension; among others, decomposition, condensation and polymerization reactions can take place in larger extension. However, for Ni/xCeZnO catalysts, an enhancement in the productivity towards hydrogen is observed. Moreover, after 20 h under reaction, Ni/20CeZnO and Ni/30CeZnO catalysts still show a H_2 yield over 20% under the substoichiometric ASR conditions (Table 2).

Post-reaction catalysts were analyzed by XRD, Raman spectroscopy and TG-TPO-MS. In all cases, after the ASR reaction, the presence of Ni^0 and NiO was determined from XRD analysis. Table 3 compiles the Ni^0 crystallite size determined from the most intense diffraction peak Ni (111) of the Ni^0 cubic phase (JCDPS 03-065-2865) for the post-reaction samples. The Ni/xCeZnO samples exhibited lower values than that determined for the Ni/ZnO sample. Moreover, as expected after the substoichiometric ASR conditions used (S/C = 1), all catalysts showed the formation of carbonaceous deposits as determined from TG-TPO-MS and Raman spectroscopy analysis. Table 3 shows the determined rate of formation of carbonaceous deposits from TG-TPO-MS analysis after 20 h under ASR. The higher amount of carbonaceous deposits was found for the bare Ni/ZnO catalyst. A decrease of the carbonaceous deposits was found for the Ni/xCeZnO catalysts when compared to the Ni/ZnO catalyst, which in turn diminished with the content of CeO_2 in the catalyst and, according the determined OSC values.

Moreover, the TPO-MS profile of evolved CO_2 during the analysis (Fig. 5) indicates that the temperature of starting the combustion of the carbonaceous deposits was lower for the Ni/xCeZnO catalysts than for the bare Ni/ZnO catalyst.

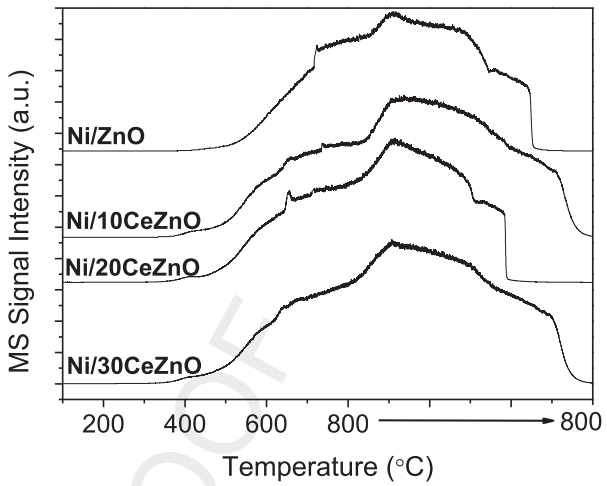

Fig. 5 – Temperature programmed oxidation (TG-TPO-MS), CO_2-profiles, of post-reaction catalysts after the substoichiometric ASR test (20 h).

Raman spectroscopy analysis was used to determine the degree of graphitization of the carbonaceous deposits by using the relative intensity of the characteristic D and G bands. The I_G/I_D values determined for the post-reaction catalysts are compiled in Table 3. The graphitization character of the carbonaceous deposits formed follows the trend: Ni/ZnO > Ni/10CeZnO > Ni/20CeZnO > Ni/30CeZnO. From the Raman analysis results it appears that, the higher is the CeO_2 content, the poorer graphitization of the carbon deposits exists. That pointing to the more graphitic nature of the deposits for the Ni/ZnO sample in agreement with the results from the TG-TPO-MS analysis.

Conclusions

Ni/xCeZnO catalysts showed a better performance under the substoichiometric ASR conditions used (S/C = 1) than the bare Ni/ZnO; the highest H_2-yield was found for the Ni/30CeZnO catalyst.

The amount of carbonaceous deposits and their graphitic nature in post-reaction ASR (S/C = 1) is lower for Ni/xCeZnO than for Ni/ZnO catalysts. The higher the CeO_2 content in Ni/xCeZnO, the lower the amount of carbonaceous deposits in the post-reaction catalyst. This is related with the OSC values that increased with the amount of CeO_2 in the catalysts.

In-situ DRIFTS-MS experiments under ESR conditions pointed to different reaction pathways over Ni/20CeZnO and Ni/ZnO catalysts; in the former the formation of acetone by-product was less favored. Thus, subsequent oligomerization reactions and carbon formation could be prevented under ESR conditions over Ni/20CeZnO respect to Ni/ZnO.

Acknowledgements

The authors thank Brazilian CAPES, CNPq, USP, LNLS support and the Spanish MICINN-FEDER MAT2014-52416-P and MAT2017-87500-P projects for financial support. Q3

Please cite this article as: Elias KFM et al., Study of Ni/CeO_2–ZnO catalysts in the production of H_2 from acetone steam reforming, International Journal of Hydrogen Energy, https://doi.org/10.1016/j.ijhydene.2018.10.191

REFERENCES

[1] Li D, Li X, Gong J. Catalytic reforming of oxygenates: state of the art and future prospects. Chem Rev 2016;116:11529–653. https://doi.org/10.1021/acs.chemrev.6b00099.

[2] Ramírez de la Piscina P, Homs N. Ethanol reformation to hydrogen, chapter 13. In: Alcoholic fuels, shelley minteer. CRC Press, Taylor&Francis Group; 2006. p. 233–48. ISBN-13: 9780849339448.

[3] Mattos LV, Jacobs G, Davis BH, Noronha FB. Production of hydrogen from ethanol: review of reaction mechanism and catalyst deactivation. Chem Rev 2012;112:4094–123. https://doi.org/10.1021/cr2000114.

[4] Montero C, Ochoa A, Castaño P, Bilbao J, Gayubo AG. Monitoring Ni^0 and coke evolution during the deactivation of a Ni/La_2O_3–αAl_2O_3 catalyst in ethanol steam reforming in a fluidized bed. J Catal 2015;331:181–92. https://doi.org/10.1016/j.jcat.2015.08.005.

[5] Navarro RM, Guil-Lopez R, Gonzalez-Carballo JM, Cubero A, Ismail AA, Al-Sayari SA, et al. Ni- and PtNi-catalysts supported on Al_2O_3 for acetone steam reforming: effect of the modification of support with Ce, La and Mg. Catal Today 2015;242:60–70. https://doi.org/10.1016/j.cattod.2014.07.036.

[6] González-Gil R, Chamorro-Burgos I, Herrera C, Larrubia MA, Laborde M, Mariño F, et al. Production of hydrogen by catalytic steam reforming of oxygenated model compounds on Ni-modified supported catalysts. simulation and experimental study. Int J Hydrogen Energy 2015;40:11217–27. https://doi.org/10.1016/j.ijhydene.2015.05.167.

[7] Esteban-Díez G, Gil MV, Pevida C, Chen D, Rubiera F. Effect of operating conditions on the sorption enhanced steam reforming of blends of acetic acid and acetone as bio-oil model compounds. Appl Energy 2016;177:579–90. https://doi.org/10.1016/j.apenergy.2016.05.149.

[8] Hu X, Zhang L, Lu G. Pruning of the surface species on Ni/Al_2O_3 catalyst to selective production of hydrogen via acetone and acetic acid steam reforming. Appl Catal A 2012;427–8:49–57. https://doi.org/10.1016/j.apcata.2012.03.029.

[9] Choi IH, Hwang KR, Lee KY, Lee IG. Catalytic steam reforming of biomass-derived acetic acid over modified $Ni/\gamma\ Al_2O_3$ for sustainable hydrogen production. Int J Hydrogen Energy 2018 (in press), https://doi.org/10.1016/j.ijhydene.2018.04.192.

[10] Ramírez de la Piscina P, Homs N. Use of biofuels to produce hydrogen (reformation processes). Chem Soc Rev 2008;37:2459–67.

[11] Kubacka A, Fernández-García M, Martínez-Arias A. Catalytic hydrogen production through WGS or steam reforming of alcohols over Cu, Ni and Co catalysts. Appl Catal A 2016;518:2–17. https://doi.org/10.1016/j.apcata.2016.01.027.

[12] a)Bednarczuk L, Ramirez de la Piscina P, Homs N. H_2-production from CO_2-assisted ethanol steam reforming: the regeneration of Ni-based catalysts. Int J Hydrogen Energy 2015;40:5256–63.
b)Bednarczuk L, Ramirez de la Piscina P, Homs N. Efficient CO_2-regeneration of Ni/Y_2O_3-La_2O_3-ZrO_2 systems used in the ethanol steam reforming for hydrogen production. Int J Hydrogen Energy 2016;41:19509–17.

[13] Pinton N, Vidal MV, Signoretto N, Martínez-Arias A, Cortés Corberán V. Ethanol steam reforming on nanostructured catalysts of Ni, Co and CeO_2: influence of synthesis method on activity, deactivation and regenerability. Catal Today 2017;296:135–43.

[14] Huang SH, Chen Zhanghai, Shen XC, Zhu ZQ, Yu K. Raman scattering of single tetrapod-like ZnO nanostructure synthesized by catalyst-free rapid evaporation. Solid State Commun 2008;145:418–22. https://doi.org/10.1016/j.ssc.2007.11.014.

[15] Kostić R R, Aškrabić S, Dohčević-Mitrović Z, Popović ZV. Low-frequency Raman scattering from CeO_2 nanoparticles. Appl Phys A: Materials Science and Processing 2008;90:679–83. https://doi.org/10.1007/s00339-007-4345-6.

[16] Dohčević-Mitrović ZD, Šćepanović MJ, Grujić-Brojčin MU, Popović ZV, Bošković SB, Matović BM, et al. The size and strain effects on the Raman spectra of $Ce_{1-x}Nd_xO_{2-\delta}$ ($0 \leq x \leq 0.25$) nanopowders. Solid State Commun 2006;137:387–90. https://doi.org/10.1016/j.ssc.2005.12.006.

[17] Rodriguez JA, Hanson JC, Frenkel AI, Kim JY, Pérez M. Experimental and theoretical studies on the reaction of H_2 with NiO: role of O vacancies and mechanism for oxide reduction. J Am Chem Soc 2002;124:346–54. https://doi.org/10.1021/ja0121080.

[18] Gonzalez-De la Cruz VM, Holgado JP, Pereniguez R, Caballero A. Morphology changes induced by strong metal-support interaction on a Ni-ceria catalytic system. J Catal 2008;257:307–14. https://doi.org/10.1016/j.jcat.2008.05.009.

[19] Ma J, Sun N, Zhang X, Zhao N, Xiao F, Wei W, et al. A short review of catalysis for CO_2 conversion. Catal Today 2009;148:221–31. https://doi.org/10.1016/j.cattod.2009.08.015.

[20] Llorca J, Homs N, Ramirez de la Piscina P. In situ DRIFT-mass spectrometry study of the ethanol steam-reforming reaction over carbonyl-derived Co/ZnO catalysts. J Catal 2004;227:556–60. https://doi.org/10.1016/j.jcat.2004.08.024.

[21] Yee A, Morrison SJ, Idriss H. A study of the reactions of ethanol on CeO_2 and Pd/CeO_2 by steady state reactions, temperature programmed desorption, and in situ FT-IR. J Catal 1999;186:279–95. https://doi.org/10.1006/jcat.1999.2563.

[22] Carriazo D, Martin C, Rives V. An FT-IR study of the adsorption of isopropanol on calcined layered double hydroxides containing isopolymolybdate. Catal Today 2007;126:153–61. https://doi.org/10.1016/j.cattod.2006.10.009.

[23] Guil JM, Homs N, Llorca J, Ramirez de la Piscina P. Microcalorimetric and infrared studies of ethanol and acetaldehyde adsorption to investigate the ethanol steam reforming on supported cobalt catalysts. J Phys Chem B 2005;109:10813–9. https://doi.org/10.1021/jp050414k.

[24] Araña J, Doña-Rodriguez JM, Garriga i Cabo C, Gonzalez-Diaz O, Herrera-Melian JA, Perez-Peña J. FTIR study of gas-phase alcohols photocatalytic degradation with TiO_2 and AC-TiO_2. Appl Catal B 2004;53:221–32. https://doi.org/10.1016/j.apcatb.2004.04.024.

[25] Carvalho DL, Borges LEP, Appel LG, Ramírez de la Piscina P, Homs N. In situ infrared spectroscopic study of the reaction pathway of the direct synthesis of n-butanol from ethanol over MgAl mixed-oxide catalysts. Catal Today 2013;213:115–21. https://doi.org/10.1016/j.cattod.2013.03.034.

[26] Ordomsky VV, Sushkevich VL, Ivanova II. Study of acetaldehyde condensation chemistry over magnesia and zirconia supported on silica. J Mol Catal A 2010;333:85–93. https://doi.org/10.1016/j.molcata.2010.10.001.

[27] de Jesus JC, Zaera F. Adsorption and thermal chemistry of acrolein and crotonaldehyde on Pt(111) surfaces. Surf Sci 1999;430:99–115. https://doi.org/10.1016/S0039-6028(99)00406-9.

[28] Singh M, Zhou N, Paul DK, Klabunde KJ. IR spectral evidence of aldol condensation: acetaldehyde adsorption over TiO_2 surface. J Catal 2008;260:371–9. https://doi.org/10.1016/j.jcat.2008.07.020.

[29] Madhavaram H, Idriss H. Acetaldehyde reactions over the uranium oxide system. J Catal 2004;224:358–69. https://doi.org/10.1016/j.jcat.2004.03.018.

[30] Hauchecorne B, Terrens D, Verbruggen S, Martens JA, Langenhove HV, Demeestere K, et al. Elucidating the photocatalytic degradation pathway of acetaldehyde: an FTIR in situ study under atmospheric conditions. Appl Catal

Please cite this article as: Elias KFM et al., Study of Ni/CeO_2–ZnO catalysts in the production of H_2 from acetone steam reforming, International Journal of Hydrogen Energy, https://doi.org/10.1016/j.ijhydene.2018.10.191

B Environ 2011;106:630–8. https://doi.org/10.1016/j.apcatb.2011.06.026.

[31] Chang Y-C, Ko A-N. Vapor phase reactions of acetaldehyde over type X zeolites. Appl Catal A 2000;190:149–55. https://doi.org/10.1016/S0926-860X(99)00293-8.

[32] Toyir J, Ramírez de la Piscina P, Homs N. Ga-promoted copper-based catalysts highly selective for methanol steam reforming to hydrogen; relation with the hydrogenation of CO_2 to methanol. Int J Hydrogen Energy 2015;40:11261–6. https://doi.org/10.1016/j.ijhydene.2015.04.039.

[33] Salvapati GS, Ramanamurty KV, Janardanarao M. Selective catalytic self-condensation of acetone. J Mol Catal 1989;54:9–30.

Please cite this article as: Elias KFM et al., Study of Ni/CeO_2–ZnO catalysts in the production of H_2 from acetone steam reforming, International Journal of Hydrogen Energy, https://doi.org/10.1016/j.ijhydene.2018.10.191